Improved Multi-body Rope Approach for Free-Form Grid Shells

Improved Multi-Body Rope Approach for Free-form grid shells*

Amedeo Manuello[1 [0000−0003−1474−0176]], Jonathan Melchiorre[1 [0000−0002−8721−8365]], Giuseppe Carlo Marano[1 [0000−0001−8472−2956]]

Department of Structural, Geotechnical and Building Engineering, Politecnico di Torino, Corso Duca degli Abruzzi, 24 - 10129. Torino, Italy.
amedeo.manuellobertetto@polito.it

Abstract. Due to their ability to provide broad, lightweight roofs with slim main structural elements, grid-shell roofing systems are becoming more and more common in contemporary engineering and design. However, their widespread and extensive use outside of high-end projects or super architecture has been constrained by their complex and expensive fabrication. In order to solve this, it has been demonstrated that the Multi-body Rope Approach (MRA) is successful in calculating structurally efficient geometries that can decrease internal stresses, which are closely related to the structural shape of gridshells. Different MRA-improving strategies are put forth in this paper: The number of various structural components needed to build a gridshell can be significantly reduced thanks to Multiple Order MRA (MO-MRA) and Repulsive Nodes MRA (RN-MRA) strategy. Due to mass production, the suggested methodology offers lower manufacturing costs as well as improved building stage management. Finally, by a Matlab code and the new approaches were tested in various case-study structures.

Keywords: Multi-body Rope Approach · Multiple Order · Grid-shell · Form-finding · Light-weight Structures

1 Introduction

There has been an increase in demand in recent years for architectural structures that provide greater internal distribution flexibility. Double-curved shells and domes have emerged as a viable option for achieving both column-free areas and complicated designs[1]. Free-form shell buildings, often referred to as curved shell structures, have drawn a lot of interest because of their distinctive and attractive features [2]. Without the need of beams, columns, or walls, shells are thin, self-supporting structures with a single or double curve that can cover large spaces. The membranous behavior, which demonstrates superior structural efficiency, is the preferred. To avoid local (buckling) and non-local (snap-through) instability issues, adequate bending stiffness must be given if

* Supported by organization x.

compressive membrane states are present. A three-dimensional grid shell is constituted of straight elements connected by nodes makes up a gridshell, a type of free-form shell construction. Gridshells thus provide a variety of structural and aesthetically pleasing advantages. They are compact, self-supporting structures that can span wide areas with the least amount of material. [3, 4]. In the 1960s and 70s [5, 6] innovative new methods for gridshell design were carried out. They produced intricate, double-curved structures using computer modeling and lightweight materials. Timber and other materials were frequently used to construct early gridshells [7] to create vast open spaces like exhibition halls, sports arenas etc. [8]. Gridshell structures are defined by the interaction between their shape and stress distribution. Because of this relationship between shape and forces, designing such structures directly, as in the case of conventional structures, is ineffective. In this scenario, the search for a suitable structural shape is critical, both for design aesthetics and for the structural efficiency. To achieve a feasible shape, it is necessary to balance the internal forces and loads acting on the structure and minimize the bending moment within the resisting elements [9]. Numerous form-finding strategies, including both physical and computational modeling techniques, have been developed over time to aid in the design of these complex structures. [10]. Among the most popular form-finding methods are the force density method [11], thrust network analysis [12], dynamic relaxation method [13], particle-spring system [14], multi-body rope approach [15], and others [16–18]. Innovating shapes and free-form structures with structural optimization is the newest trend in structural design research [19–23]. The improved Multi-body Rope Approach (i-MRA), a novel advancement of the form-finding technique created exclusively for gridshells, is presented in this study. The Multi-body Rope Approach (i-MRA) is built upon by the MRA technique [15]. A net of masses connected by flexible ropes or cables serves as the MRA representation of a structure. As a result, the structure's geometry can be defined by reducing bending moments and stresses. [24]. The MRA method minimizes the eccentricity of applied compression forces to design the structural geometry [25]. By including strategies that optimize the structural geometry for both structural and automation of the construction process, the i-MRA method outperforms MRA. The i-MRA has two main advancements: (i) Multiple Orders MRA (MO-MRA): reduces the variety of structural component types; (ii) Repulsive Nodes MRA (RN-MRA): creates a repulsive force field for the dynamic model. Different examples of increasing complexity were used to demonstrate the i-MRA method's ability to produce the best structural geometry. A structural analysis of the structures obtained by basic MRA and i-MRA was conducted in order to confirm that the geometries obtained by the new method proposed did not have any significant structural disadvantages (in terms of internal solicitations) compared to those calculated by pure form-finding methods. Finite element analyses were carried out for this purpose utilizing the SOFiSTiK [26].

2 Methods

2.1 The Basic MRA Method

The Multibody Rope Approach (MRA), developed by [15], is an original technique for figuring out the shape of gridshell structures, even for extremely complicated geometries and under any forming load. The D'Alembert's principle is used in MRA to iteratively determine the final equilibrium configuration for each node using a dynamic model of falling bodies in the space and time domains. An inverted image of the hanging net is the structure's final equilibrium configuration (also known as the funicular configuration). MRA makes the same assumption as particle-spring models on the localization of the nodes' self-weight and rope loads. In contrast to these strategies, MRA models the hanging network using ropes. Unlike the spring-particle (SP) and dynamic relaxation (DR) approaches, MRA's system of forces acting on individual nodes is separate from those in those techniques. No force is exerted if the distance between the ends is less than the rope's fixed length (l_rope). The forces F exerted on the end nodes can be represented as follows by defining l as the distance between the two ends of the rope and k as its axial stiffness:

$$\begin{cases} F_{rope} = 0 & \text{if} \quad l < l_{rope} \\ F_{rope} = k(l - l_{rope}) & \text{if} \quad l \geq l_{rope} \end{cases} \tag{1}$$

The MRA technique generally assumes very high stiffness levels in order to reduce axial deformations. Consider a generic node i in the nodes and ropes structural network that has a mass of m_i. The node i is roped together with n_i other nodes. The equilibrium equation looks like this if node i is subject to an external load p_i:

$$\vec{R}_i = \vec{p}_i + \sum_{j=1}^{n_i} \vec{F}_{rope,ji} + \vec{F}_i^I + \vec{F}_i^{II} = 0 \tag{2}$$

In this equation, the vector $\vec{R}i$ represents the net force acting on node i, wwhich is the result of the addition of various forces, such as the applied load p_i and the forces transmitted by the ropes holding the node in place. $\vec{F}rope, ji$, the inertial force $\vec{F}_i^{II}$, and the damping force $\vec{F}_i^I$. The magnitude of the inertial force $\vec{F}_i^{II}$ can be calculated as the product of the node's mass m_i and the magnitude of the acceleration vector $\vec{a}_i$, with the direction of the inertial force being opposite to the direction of node acceleration. Expressing the position of the generic node i as $\vec{u}_i = (x_i, y_i, z_i)$, the velocity and the acceleration can be obtained by deriving the position in time, as in the relations (3).

$$\vec{v}_i = \dot{\vec{u}}_i = (\dot{x}_i, \dot{y}_i, \dot{z}_i) \qquad \vec{a}_i = \ddot{\vec{u}}_i = (\ddot{x}_i, \ddot{y}_i, \ddot{z}_i) \tag{3}$$

Finally, the equilibrium equation can be projected in the three space dimensions, obtaining the system of equation (4).

$$\begin{cases} p_{ix} + \sum_{j=1}^{n_i} \left\{ \frac{(x_j - x_i)}{l_{ji}} \cdot F_{rope} \right\} - c_i \cdot \dot{x}_i - m_i \cdot \ddot{x}_i = 0 \\ p_{iy} + \sum_{j=1}^{n_i} \left\{ \frac{(y_j - y_i)}{l_{ji}} \cdot F_{rope} \right\} - c_i \cdot \dot{y}_i - m_i \cdot \ddot{y}_i = 0 \\ p_{iz} + \sum_{j=1}^{n_i} \left\{ \frac{(z_j - z_i)}{l_{ji}} \cdot F_{rope} \right\} - c_i \cdot \dot{z}_i - m_i \cdot \ddot{z}_i = 0 \end{cases} \tag{4}$$

The system may be resolved taking into account a time increment Δt. By knowing the position, velocity, and acceleration of each node at time t, these quantities can be determined at the next instant, $t + \Delta t$. A coefficient C_3 can is defined as a function of the known node positions at time t^*.

$$C_3 = \vec{p}_i + \sum_{j=1}^{n_i} \left\{ k \cdot \vec{F}_{rope,ji} \right\} \tag{5}$$

The coefficient C_3 depends solely on the position of the nodes at time t^*, and it defines the vector F_{rope}.

$$\ddot{\vec{u}} + \frac{c}{m} \dot{\vec{u}} = C_3 \tag{6}$$

In addition, the natural frequency of the system ω_n and critical damping ζ can be defined:

$$\omega_n = \sqrt{\frac{k}{m}} \tag{7}$$

$$\zeta = \frac{c}{2\omega_n m} \tag{8}$$

k is the stiffness, m is the mass, and c is the damping coefficient of the system. The natural frequency ω_n represents the frequency at which the system vibrates when it is not subjected to any external forces. The critical damping ζ is the damping coefficient value that results in the system being critically damped, which means that it returns to its equilibrium state as quickly as possible without oscillating.

$$\ddot{\vec{u}} + 2\omega_n \zeta \dot{\vec{u}} = C_3 \tag{9}$$

By adding the specific solution to the corresponding homogeneous differential equation, which is denoted by the following expression:

$$\vec{u}(t) = C_1 e^{-2\omega_n \zeta} + C_2 + \frac{C_3}{2\omega_n \zeta} t \tag{10}$$

The coefficients C_1 and C_2 can be calculated using the system's initial conditions. In this situation, they can be derived by using the nodes' locations and velocities at the previous instant $t - \Delta t$, as shown in the following equations:

$$C_1 = -\frac{2\omega_n \zeta \dot{\vec{u}}_{(t-\Delta t)} - C_3}{(2\omega_n \zeta)^2} \tag{11}$$

$$C_2 = -\frac{(2\omega_n\zeta)^2\vec{u}_{(t-\Delta t)} + 2\omega_n\zeta\dot{\vec{u}}_{(t-\Delta t)} - C_3}{(2\omega_n\zeta)^2} \tag{12}$$

The coefficients C_1, C_2, and C_3 in the solution rely on the nodes' locations, speeds, and accelerations at the preceding time instant.

$$\dot{\vec{u}}_t = \frac{\vec{u}_t - \vec{u}_{t-\Delta t}}{\Delta t} \tag{13}$$

Finally, the acceleration $\ddot{\vec{u}}_t$ can be calculated by subtracting the two velocities and multiplying the result by the time interval Δt.

$$\ddot{\vec{u}}_t = \frac{\ddot{\vec{u}}_t - \ddot{\vec{u}}_{t-\Delta t}}{\Delta t} \tag{14}$$

The suggested technique is made to determine the final configuration of a gridshell from its original mesh, which symbolizes the net's starting state. Until an equilibrium configuration is reached that represents the best structural geometry in relation to the applied force field $\vec{p}$, this process is repeated. The structural shape is a function of the nodal masses m, the system stiffness k, damping parameters c, the rope slack coefficient ρ, and the applied force field $\vec{p}$. The slack coefficient ρ is defined as the ratio of the initial distance between nodes to the target length of the ropes, as shown in the following equation.

$$\rho_{ij} = \frac{l_{rope}}{\vec{u}_i(0) - \vec{u}_j(0)} \tag{15}$$

Structural elements are divided into three groups according to their length: those with a length less than l_{rope} are called *loose elements*, those with a length greater than l_{rope} are called *over elements*, and those with a length equal to l_{rope} are referred to as *target elements*.

2.2 Shape and Constructability the Improved-MRA

To cut down on the variety of structural components obtained by MRA, the Multiple Order based on the MRA method is used, the new target in to reduce the number of *loose elements* in the final configuration. This is accomplished without materially changing the structural geometry by introducing additional families of shorter-length ropes that are positioned in the areas where the loose parts are found. The gridshell geometry is first calculated using traditional MRA with a goal length of $l_{rope,1}$. A new rope family with a shorter length will be created after the final equilibrium arrangement is achieved ($l_{rope,2} < l_{rope,1}$) and the geometric configuration is iteratively calculated.

$$\begin{cases} F_{rope} = 0 & \text{if} \quad l < l_{rope,2} \\ F_{rope} = k(l - l_{rope,2}) & \text{if} \quad l_{rope,2} < l \leq (l_{rope,1} - l_{rope,2}) + l_{rope,2} \\ F_{rope} = 0 & \text{if} \quad \gamma(l_{rope,1} - l_{rope,2}) + l_{rope,2} < l < l_{rope,1} \\ F_{rope} = k(l - l_{rope,1}) & \text{if} \quad l \geq l_{rope,1} \end{cases} \tag{16}$$

The γ coefficient can be modulated to obtain different geometric configurations by preferring ropes of length $l_{rope,1}$ or $l_{rope,2}$, and it was found that setting $\gamma = \frac{2}{3}$ yields sufficient results. It is possible to introduce new families of elements and set a target length of $l_{rope,3} < l_{rope,2}$ for any remaining *loose elements*. At the same time, the Repulsive Nodes MRA is a method designed to reduce the number of *loose elements* generated by applying the basic MRA. The basic idea is to introduce a repulsive force field $\vec{q}$ between the nodes of the geometric configuration obtained through the use of MRA. This force field $\vec{q}$ is introduced after the final equilibrium configuration is established using the MRA, which requires a new iterative computation process to determine the new equilibrium condition.

$$\vec{R}_i = \vec{p}_i + \vec{q}_i + \sum_{j=1}^{n_i} \left\{ k \cdot \vec{F}_{rope,ji} \right\} - c_i \cdot \vec{v}_i - m_i \cdot \vec{a}_i = 0 \tag{17}$$

Equation (17) introduces the repulsive force field $\vec{q}$ to each node i connected to slack ropes. This force field $\vec{q}$ is linearly proportional to the difference between the target length l_{rope} and the distance between nodes connected by a slack rope l_{ij}. To calculate the repulsive force field $\vec{q}$, Equation (18) can be used, where k_{rep} is the proportionality constant that connects the modulus of the repulsive force to the distance between nodes i and j.

$$q_i = -k_{rep}(l_{rope} - l_{ij}) \tag{18}$$

The RN-MRA method has been observed to converge faster to an equilibrium configuration when a smaller value of k_{rep} is chosen relative to k. However, the designer has the flexibility to choose the value of k_{rep} based on the design situation. Ideally, RN-MRA should be applied to models with few *loose elements* relative to the number of tensioned ones, and where their length is close to the target length l_{rope}.

3 Application and results

This section presents two main applications of the suggested technique to structural geometries with increasing levels of complexity. The comparison demonstrates that the i-MRA can lower gridshell structure realization costs while maintaining the structurally ideal solution obtained by a pure form-finding method (basic MRA). Overall, it is demonstrated that the suggested approach is successful in delivering structural solutions that are both practical and simple to build. The first application regards the structural geometry of a square gridshell defined using the MRA method applied to a square mesh with a side of 15 meters and lines placed in an orthogonal grid linking nodes at a distance of $l_{ij} = 1.25m$. The limitations are depicted as triangular points, and the construction is intended to be confined exclusively in the corners of the square plan. The second kind of application example seeks to assess the performance of the suggested strategy in a very broad scenario. When using the method, a base plan with a free-form

curve as its definition is taken into account, and a parametric design tool is used to generate the mesh automatically. The quadrangular mesh and the mesh made up of hexagonal and pentagonal elements are the two types of meshes that are the subject of the analysis. As a result, this is the most complex application of MRA because the suggested goal is to produce equal structural pieces from a geometry made up of various elements. The edges in both of the meshes shown in this section have an average length of roughly 1.50 meters.

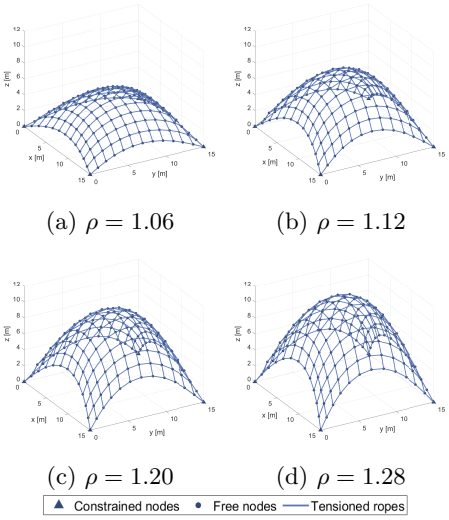

(a) $\rho = 1.06$ (b) $\rho = 1.12$

(c) $\rho = 1.20$ (d) $\rho = 1.28$

Fig. 1: MRA application on corner constrained square-plan structure for different slack coefficients ρ.

Nevertheless, the components of the quadrangular mesh in Figure 2*a* range in length from approximately 0.80 m to 2.30 m, resulting in a significant amount of variety in the starting pieces. When structural elements' final lengths depart from the desired length, red is used to show them $L_{rope} = 1.78m$ (*loose ropes*). Due to the anomalies in the basic geometry, these components make up more than 13% of the 750 structural elements that make up the gridshell. To build the real construction, more than 100 distinct types of structural components are needed. Construction phase management may be more problematic than in the preceding examples, despite the fact that this may be doable on the construction site for simple and complicated structural shapes. However, Figures illustrate the structural configuration attained by utilizing the i-MRA described in this paper 2*b* and 2*d*. This example shows a substantial improvement. The method allowed for the calculation of a structural geometry that only required the use of 7 different lengths for structural component types $L_{rope} = [1.78; 1.58; 1.45; 1.35; 1.25; 1.15]m$. This amazing result shows how the

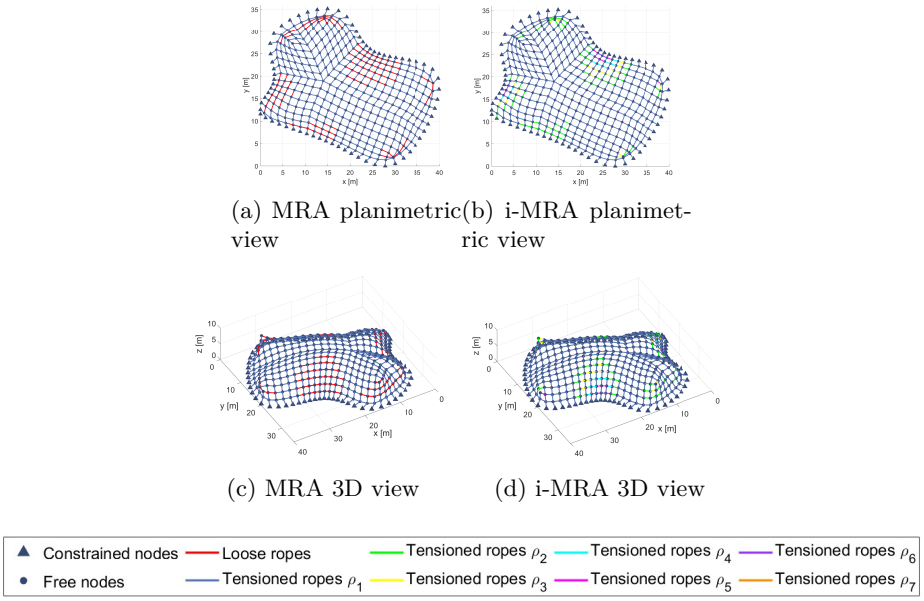

Fig. 2: Comparison between MRA and i-MRA on a free-form structure with quadrangular mesh.

methods described in Section 2 can significantly lessen building complexity. The results of the structural evaluations shown in the Figures show that the modifications to the structural geometry made possible by i-MRA did not significantly raise stresses. With the introduction of i-MRA, the number of structural elements used dropped from over 100 to just 6. The imposed Von Mises stresses increased by less than 0.7 percent, which is a minimal rise, despite the geometric alterations made. Additionally, the work's construction complexity—as measured by the various structural elements used—was reduced by nearly 20 times.

4 Conclusions

In this paper, a form-finding technique for gridshell structures is presented. The approach expands on the Multi-body Rope Approach (MRA) created by [15]. Different improvement strategies are suggested for the fundamental MRA in order to further limit the complexity of structural construction management and lessen computing effort. The first method reduces the variety of structural elements needed to build the estimated structures by designating groups of structural parts with identical lengths. In the second method, a repulsive force field is applied to the dynamic model, allowing for minute geometry tweaks to reduce the amount of structural components that do not fall into the predefined groups.

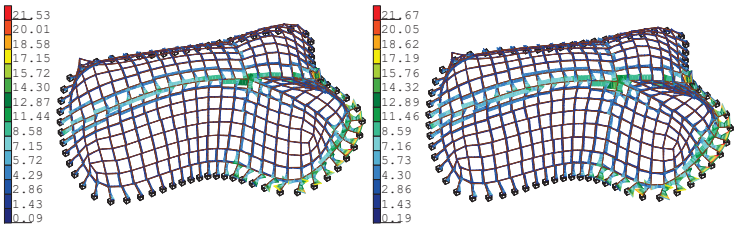

(a) MRA: $|\sigma^{VM}|_{max} = 21.53kPa$ (b) i-MRA: $|\sigma^{VM}|_{max} = 21.67kPa$

Fig. 3: Structural analysis performed on the structures obtained by applying basic MRA (left) and i-MRA (right) on the application example with quadrangular mesh. Comparison in terms of Von Mises stress [kPa].

Application examples with varying degrees of complexity were used to test the efficiency of the suggested strategy. The findings demonstrated that, particularly as the geometric complexity of the structure rises, the i-MRA technique significantly lowers the number of structural components needed.

References

1. J. N. Richardson, S. Adriaenssens, R. F. Coelho, P. Bouillard, Coupled form-finding and grid optimization approach for single layer grid shells, Engineering structures 52 (2013) 230–239.
2. J. Chilton, C.-C. Chuang, Rooted in nature: aesthetics, geometry and structure in the shells of heinz isler, Nexus Network Journal 19 (3) (2017) 763–785.
3. X. Tellier, Bundling elastic gridshells with alignable nets. part ii: Form-finding, Automation in Construction 141 (2022) 104292.
4. V. Tomei, E. Grande, M. Imbimbo, Design optimization of gridshells equipped with pre-tensioned rods, Journal of Building Engineering 52 (2022) 104407.
5. E. Happold, Philosophy of design with particular respect to buildings, Structural Engineering: History and development (1997).
6. B. Addis, D. Walker, Happold: The confidence to build, Taylor & Francis, 2005.
7. I. Liddell, Frei otto and the development of gridshells, Case Studies in Structural Engineering 4 (2015) 39–49.
8. W. Pan, M. Turrin, C. Louter, S. Sariyildiz, Y. Sun, Integrating multi-functional space and long-span structure in the early design stage of indoor sports arenas by using parametric modelling and multi-objective optimization, Journal of Building Engineering 22 (2019) 464–485.
9. L. Gründig, E. Moncrieff, P. Singer, D. Ströbel, A history of the principal developments and applications of the force density method in germany 1970–1999, in: Proceedings of IASS-IACM 2000 Fourth International Colloquium on Computation of Shell & Spatial Structures, Chania-Crete, Greece, 2000.
10. R. Mesnil, C. Douthe, O. Baverel, T. Gobin, Form finding of nexorades using the translations method, Automation in Construction 95 (2018) 142–154.

11. H.-J. Schek, The force density method for form finding and computation of general networks, Computer methods in applied mechanics and engineering 3 (1) (1974) 115–134.
12. J. R. H. Otter, A. C. Cassell, R. E. Hobbs, POISSON, Dynamic relaxation, Proceedings of the Institution of Civil Engineers 35 (4) (1966) 633–656.
13. P. Block, J. Ochsendorf, Thrust network analysis: a new methodology for three-dimensional equilibrium, Journal of the International Association for shell and spatial structures 48 (3) (2007) 167–173.
14. A. Kilian, J. Ochsendorf, Particle-spring systems for structural form finding, Journal of the international association for shell and spatial structures 46 (2) (2005) 77–84.
15. A. Manuello, Multi-body rope approach for grid shells: form-finding and imperfection sensitivity, Engineering Structures 221 (2020) 111029.
16. I. M. Rian, M. Sassone, S. Asayama, From fractal geometry to architecture: Designing a grid-shell-like structure using the takagi–landsberg surface, Computer-Aided Design 98 (2018) 40–53.
17. Z. Zhao, D. Yu, T. Zhang, N. Zhang, H. Liu, B. Liang, L. Xian, Efficient form-finding algorithm for freeform grid structures based on inverse hanging method, Journal of Building Engineering 46 (2022) 103746.
18. W. Huang, C. Wu, J. Hu, W. Gao, Weaving structure: A bending-active gridshell for freeform fabrication, Automation in Construction 136 (2022) 104184.
19. K. Yamamoto, T. Ogawa, M. Fujimoto, C. Lazaro, T. Takeuchi, S.-D. Xue, P.-S. Chen, S. Kato, State-of-the-art for optimization of forms and strength for reticulated shells, in: IASS Annual Symposium; IASS-APCS: London, UK, 2012.
20. S. Adriaenssens, P. Block, D. Veenendaal, C. Williams, Shell structures for architecture: form finding and optimization, Routledge, 2014.
21. J. Melchiorre, A. Manuello, F. Marmo, S. Adriaenssens, G. Marano, Differential formulation and numerical solution for elastic arches with variable curvature and tapered cross-sections, European Journal of Mechanics-A/Solids 97 (2023) 104757.
22. L. Bouhaya, O. Baverel, J.-F. Caron, Optimization of gridshell bar orientation using a simplified genetic approach, Structural and Multidisciplinary Optimization 50 (2014) 839–848.
23. F. Marmo, C. Demartino, G. Candela, C. Sulpizio, B. Briseghella, R. Spagnuolo, Y. Xiao, I. Vanzi, L. Rosati, On the form of the musmeci's bridge over the basento river, Engineering Structures 191 (2019) 658–673.
24. A. M. Bertetto, F. Riberi, Form-finding of pierced vaults and digital fabrication of scaled prototype, Curved and Layered Structures 8 (1) (2021) 210–224.
25. A. Manuello, J. Melchiorre, L. Sardone, G. C. Marano, Multi-body rope approach for the form-finding of shape optimized grid shell structures, in: Proceedings of the 15th World Congress on Computational Mechanics, 2022.
26. SOFiSTiK, Text Editor 2023, Flataustr. 14, 90411 Nuremberg, 2022.
URL https://www.https://www.sofistik.com